

The physico-chemical properties and sorption potentials of snail shell particulates, chitin, chitosan, and oxalic acid modified chitosan from *achatina fulica* shell

Daniel Okey Ochi^{1,2*} , Akinpelu Kamoru Babayemi² 

¹Department of Chemical Engineering Technology, Auchu Polytechnic, Auchu, NIGERIA

²Department of Chemical Engineering, Chukwuemeka Odumegwu Ojukwu University, Uli, Anambra State, NIGERIA

*Corresponding Author: ochidanielokey@gmail.com

Citation: Ochi, D. O., & Babayemi, A. K. (2023). The physico-chemical properties and sorption potentials of snail shell particulates, chitin, chitosan, and oxalic acid modified chitosan from *achatina fulica* shell. *European Journal of Sustainable Development Research*, 7(4), em0232. <https://doi.org/10.29333/ejosdr/13476>

ARTICLE INFO

Received: 02 Jan. 2023

Accepted: 26 Jun. 2023

ABSTRACT

The purpose of the research was to compare the properties of snail shell particulate (SSP) and its derivatives to those of commercial chitosan (CC) as potential adsorbents. Chitin (CT) was synthesized by deproteinizing and demineralizing SSP with dilute sodium hydroxide (NaOH) and hydrochloric acid (HCl) solutions, respectively. Chitosan (CH) was prepared by partially deacetylating CT with concentrated NaOH. The extracted CH was modified with 10.00% (w/v) oxalic acid (CH_{ox}). Energy dispersive X-Ray (EDAX), Fourier transform infrared (FTIR), Brunauer-Emmett-Teller (BET), scanning electron microscopy (SEM), and chromium adsorption were used to characterize the materials. FTIR spectra of CT and CH materials showed the presence alkyne, nitrile, primary and secondary amines/amides groups with 83.98% as the degree of deacetylation. The spectra of EDAX of CT and CH samples showcased predominant peaks, which correspond to calcium, oxygen, yttrium, and silver. SEM images showed tight, porous, and fractured surface for CT and CH materials unlike the snail shell and CC. BET surface area of the adsorbents were in the increasing order of CT<CC<CH_{ox}<SSP<CH. CH has a greater surface area of 362.32 m²/g and a mesoporosity of 71.41%. However CH_{ox} with moisture content 1.52%, bulk density of 0.58 g/cm³, ash content (AC) 0.47% and pH 10.24, has better advantage to be used as biosorbent compared to CC with moisture content 1.08%, bulk density of 0.49 g/cm³, AC 0.87% and pH 8.58. CH_{ox} had a higher chromium adsorption of 80.4 mg/g at a concentration of 150 mg/L, while having a relatively smaller surface area of 325.38 m²/g (68.36% mesoporosity). The potential removal techniques include ionic interaction between chromium ion and functional groups and surface adsorption due to the textural characteristics of adsorbent samples. When compared to CC, snail shell particle and its derivatives are potential good adsorbents.

Keywords: adsorbent, snail shell, chitin, chitosan, oxalic, characterization

INTRODUCTION

The preparation and characterization of cost effective biosorbents for the remediation of contaminated effluents (wastewater) is becoming more appealing and efficient (da Silva Alves et al., 2021). Among many other products, chitosan (CH) is promising alternative for heavy metal and other water contaminating effluent removal (Upadhyay et al., 2021). CH can be made from the shells of shrimp, prawns, crabs, insects, and other crustaceans and used for water treatment, wound healing, and other purposes (Sirajudheen et al., 2021). Because of their low cost and high content of amino and hydroxyl groups, CH from gastropoda is effective biosorbent that can enhance the removal of different aquatic contaminants via chemical chelation, electrostatic and ion exchange interactions (Keshvaridoostchokami et al., 2021).

Gastropoda is a wide taxonomic family of invertebrates that includes snails and slugs. This category includes all types of snails and slugs, as well as those found in the sea, freshwater, and on land. There are a large number of freshwater limpets, freshwater snails, land snails, and sea snails (Hamli et al., 2019). In terms of the overall number of species, the gastropoda are the class with the second-highest number of species names, after insects. The gastropoda class is the most diverse in the phylum mollusca, with 65,000 to 80,000 extant snail and slug species (Gulbis, 2019). Gastropods are among the greatest potential choices utilized in heavy metal biomonitoring investigations. The synthesis and characterization of cheap biosorbents from gastropods for the treatment of polluted effluents (wastewater) has improved in efficiency (Nguyen et al., 2023). Among many other products,

CH is promising alternative for heavy metal and other water contaminating effluent removal (Zhang et al., 2021).

Heavy metals in waters and biota suggest natural or anthropogenic sources linked to industry and domestic effluents (Singh et al., 2022). To extract chitin (CT), crustaceans' exoskeletons, such as shrimp shells, crab shells, fish scales, gastropod shells, and operculum, can be exploited.

CT is a polysaccharide composed of N-acetylglucosamine residues that are connected together by β -1,4-glycosidic bonds. CT is found in sponges, corals, and mollusks, and is the primary component of fungal walls and arthropod shells (crustaceans, insects, and arachnids). CT, for example, is nature's second most abundant biopolymer after cellulose as a working estimate for annual turnover ranges 1010-1011 tonnes (Vinod et al., 2020). However, it is mostly acquired for scientific and industrial uses from marine invertebrates like as crabs, shrimps, lobsters, and krill. CT's characteristics are determined by where it comes from. CT used in medical device manufacturing must come from certified, regulated fisheries and be adequately cleansed (Sabir et al., 2019). A simple pyrolysis procedure was employed to make an alternative, eco-friendly, and relatively cheaper adsorbent out of CT. The adsorbent was termed CT derived biochar, and it was used to treat colored effluents containing methyl violet dye (MV) Zazycki et al. (2019). CT and its derivative CH are found naturally in the shells of all crustaceans and in the exoskeletons of all insects.

Due to its distinctive properties, such as biocompatibility, biodegradability, non-toxicity, and adsorptive capacity, CH has been widely used in a variety of industries, including food biotechnology, biomedicine, water treatment, cosmetics, and pharmaceuticals (Morin-Crini et al., 2019). As a result, it's used in a wide range of applications, including water treatment and seed treatment. The seed treatment is the application of biological, physical and chemical agents like fungicide or insecticide to seeds in order to protect, improve crop performance and disinfect them from seed-borne or soil-borne pathogenic organisms and storage insects. The treatment of seeds with CH or hydro-priming has shown to significantly improve seedling emergence in the cold by 29.00%. Seeds treatment with CH increases chitinase and glucanase activities in both seeds and seedlings thereby protecting seedlings from fungal disease under cold and wet environment (Huang et al., 2021; Samarah et al., 2020). For dye and heavy metals adsorption, CH-based adsorbents have gotten a lot of interest. Many variations of this polysaccharide have been studied in order to increase CH's adsorption qualities, as well as its mechanical and physical properties. CH, a derivative of CT, has just been validated as a yet another alternative adsorbent for hazardous metals found in polluted water. CH's ability to absorb a wide variety of heavy metals is determined by its crystallinity, water attraction, and degree of deacetylation (DD). The important research topics connected to CH and its derivatives for use in dye and heavy metal removal from water are discussed by researchers (Ahmed et al., 2020; Vakili et al., 2019).

CH is modified to improve its original properties, making it more appropriate for adsorption of various contaminants. Chemical and physical changes of raw CH, such as cross-linking, grafting, and impregnation of the CH backbone, have

yielded a variety of CH derivatives (Chin et al., 2022). A better understanding of these variations and their affinity for various types of pollutants will aid future study in addressing knowledge gaps in this field. This study allows researchers to better investigate the potential of CH-derived adsorbents for the removal of a wide range of contaminants. Its chemical and physical modification process derivatives have outstanding qualities for a wide range of applications to fulfil expanding demands. Replacement reactions, chain elongation, and depolymerization are examples of chemical modifications, while physical modifications result in polymeric forms such as powders, nanoparticles, and gels (Francis et al., 2021).

Heavy metals have been introduced to natural, aquatic, and terrestrial ecosystems due to urbanization and industrialization, resulting to high levels of environmental contamination today. These heavy metals are non-biodegradable, meaning they do not decompose or disintegrate even after a long period, and their presence in streams and lakes promotes bioaccumulation in living things, resulting in health issues in plants, animals and human (Khorshidi et al., 2021). Reverse osmosis, ion exchange, solvent extraction, chemical precipitation, and adsorption have all been proposed as ways for treating heavy metal-polluted wastewater (Thasneema et al., 2020).

The giant African land snail shell has only recently gained attention as a CH feedstock for the removal of organic and heavy metal pollutants. There has not been any research on the comparison of the physiochemical characteristics of commercial chitosan (CC), extracted CH materials, and raw Auchi snail shell particulates (SSPs) in relation to their ability to adsorb chromium ions from wastewater, though. Therefore, this study was a new attempt to compare the removal of chromium ions from wastewater by CC and CH extracted from auchi *achatina fulica*. In order to treat wastewater and contribute to sustainable development objectives, this work systematically encourages the synthesis of indigenous adsorbents. In the present work, CH was prepared from snail shell, modified, characterized and compared with CC as potential adsorbent. The modification of CH using oxalic acid is to improve its physico-chemical and mechanical properties for wide applications.

MATERIALS AND METHODS

The chemicals used in this work were all analytical grades from Sigma Aldrich in Germany and was used as received. Some of the chemicals were sodium hydroxide (NaOH) (98.00%) and hydrochloric acid (HCl) (99.00%) for the preparation of CH from snail shells as well as oxalic acid dehydrate (99.90%) for CH modification. Distilled water was used to wash samples and prepare aqueous solutions.

Pre-Treatment and Synthesis of Chitosan

Achatina fulica (snail shell) was used as the raw materials for this study. The agricultural waste was collected from a disposal outlet in Auchi kingdom, Etsako West Local Government Area, Edo State. The samples were crushed with mortar and pestle, and then washed before being oven dried for 12 hours at 105 °C. The samples were ground into smaller

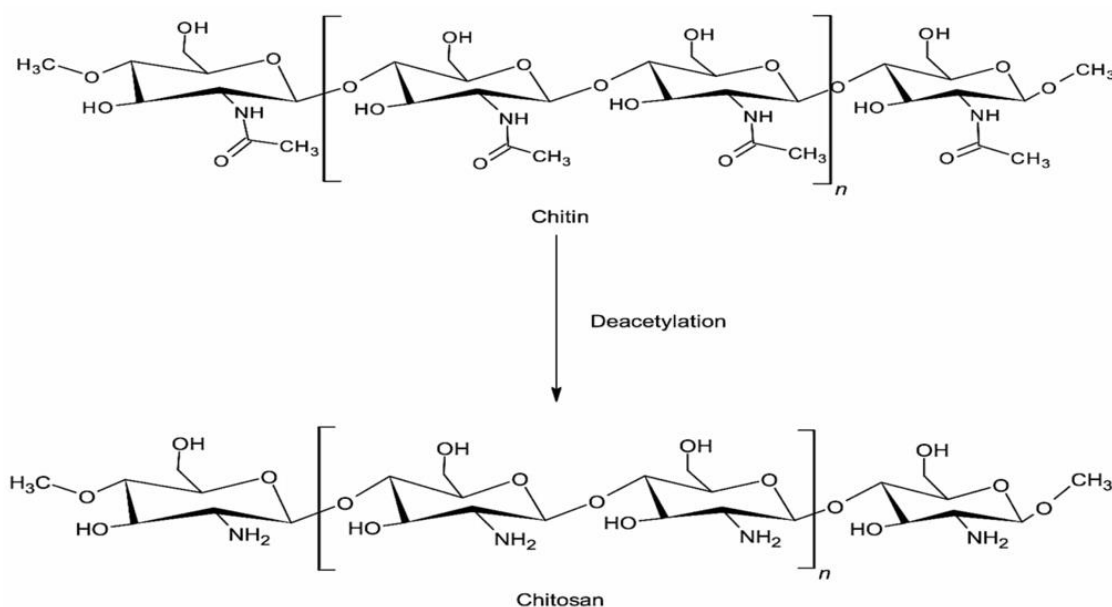


Figure 1. Conversion of chitin to chitosan by alkaline deacetylation process (Yadav et al., 2019)

pieces with a grinding machine. They were sieved to 0.150 mm particle size (Oyekunle & Omoleye, 2019a).

Two kilograms of pretreated achatina snail shells were converted into CH through deproteinization, demineralization, and deacetylation processes. Deproteinization was carried by immersing the dried, pulverized shells in a 1 M NaOH solution for six hours at 25 °C, proteins were removed. The solution was stirred at 125 rpm with the mass-to-solution ratio set to 1:6 (w/v or g/ml). The solid was filtered and then washed with distilled water to remove rid of NaOH and bring pH up to 7.0 (Wang & Zhuang, 2022).

Demineralization was achieved by immersing the deproteinized snail shell in a 5.00% (v/v) HCl solution to remove minerals, primarily calcium carbonate (Masselin et al., 2021). The mass-to-solution ratio was maintained at 1:6 (w/v), and the mixture was agitated for 30 minutes at 150 rpm at room temperature (25 °C). The demineralized shells (CTs) were then filtered and rinsed with distilled water to remove any leftover acid and bring pH to 7.0. CT was then dried in a hot air oven at 90 °C for two hours (Oyekunle & Omoleye, 2019b).

Deacetylation of CT is defined as removal of acetyl groups from CT and replacing them with reactive amino groups (NH₂). DD determines the number of free amino groups in the structure. Deacetylation is the conversion of N-acetyl groups in CT to amino groups (Hahn et al., 2020). Because glycosidic bonds are known to be acid-sensitive, the use of concentrated alkali is the most prevalent method of CT deacetylation (Hossain & Uddin, 2020). Although total removal of the acetyl groups has not been reported but repeated application of NaOH to CT can result in deacetylation of up to 98.00%. NaOH concentration, reaction temperature and time are all factors that influence the process efficiency (Masselin et al., 2021). CT was deacetylated for one hour in a water bath by mixing it with a 50.00% (w/v) concentrated NaOH solution at a solid/liquid ratio of 1:10 (g/ml), agitation at 150 rpm, and a temperature of 80 °C, as shown in **Figure 1**.

The resulting CH was filtered, washed with distilled water, and then dried in an oven for two hours at 102 °C (Wang & Zhuang, 2022). The percentage yield (Y) of the synthesized CH is evaluated, as follows:

$$\% \text{ Chitosan yield}(Y) = \frac{\text{weight of chitosan}(g)}{\text{weight of snail shell}(g)} \times \frac{100}{1}$$

Chemical Modification of Chitosan

For chemical modification, 20 g of CH was mixed with a 100 ml 10.00% (w/v) oxalic acid solution, and the mixture was continuously stirred for 60 minutes at 150 rpm and 50 °C using a magnetic stirrer. At room temperature, CH-oxalic acid combination generated a viscous whitish gel. The mixture was washed repeatedly with distilled water until it attained a pH value of seven and dried at 30 °C after 24 hours (Negm et al., 2020). The mixture was washed with distilled water after soaking it for two hours in a 0.50% (w/v) NaOH solution. Finally, it was dried for two hours in an oven at 105 °C (Rathore et al., 2021).

Physico-Chemical Characterization of Synthesized Adsorbents

The pH of the adsorbent samples was evaluated using ASTM E70-19 2019, the bulk density (ρ_s) of the samples was determined using the tampering approach according to Gao et al. (2019), the bulk density was determined, as follows:

$$\text{Bulk density}(\rho_s) = \frac{\text{mass of adsorbent}, M_s(g)}{\text{volume of adsorbent}, V_s(\text{cm}^3)}$$

The moisture content of the samples was determined at 105 °C using the method defined in ASTM D2216-19, 2019. The weight loss was used to measure the percentage moisture content of the sample, as follows:

$$\%X = \frac{M - M_1}{M} \times \frac{100}{1},$$

where %X is percentage of moisture in the sample, M is weight of wet sample (grams), and M₁ is weight of dry sample (grams).

$$\text{Dry matter}(\%) = \frac{\text{Oven dry weight}(g)}{\text{Initial sample weight}(g)} \times 100.$$

The water binding capacity (WBC) of the samples was measured to determine their textural nature. WBC of the adsorbent materials was determined using the method of (Fadhil & Mous, 2021). WBC was calculated, as follows:

$$WBC (\%) = \frac{\text{Waterbound}(g)}{\text{Initialsampleweight}(g)} \times \frac{100}{1}$$

The ash content (AC) of the adsorbents was determined by using the method of ElNasri et al. (2022). AC is calculated, as follows:

$$\%AC = \frac{M_1}{M \times (100 - X) / 100} \times \frac{100}{1} = \frac{\text{Wt of ash}}{\text{Wt of Original sample}} \times \frac{100}{1}$$

where M is the mass of the sample taken for test, M_1 is mass of ash, and X is percentage of moisture content present in adsorbent.

Fourier Transform Infrared Analysis of Chitosan

To characterize SSP and its derivatives, a Fourier transform infrared (FTIR) spectrophotometer (SHIMADZU, Model: IR affinity) was used. FTIR ranged from 4,000 to 400 cm^{-1} , with a resolution of 4 cm^{-1} . 0.20 g of the granulated adsorbent sample was encapsulated in 200 mg of KBr (sigma).

Scanning Electron Microscopy

A Karl Zeiss scanning electron microscope was used to analyze the surface morphology and texture of CH samples (SEM). The sample was placed on a metallic disk, spread onto the carbon adhesive tape, and gold-coated before inspection. SEM images were obtained at various magnifications.

Energy Dispersive X-Ray Analysis

An energy dispersive X-Ray (EDAX) analysis was performed on the prepared adsorbents to ascertain the elemental compositions of CH materials using BRUKER EDX two-dimensional VANTEC-500 detector.

Determination of Surface Area by Brunauer-Emmett-Teller Technique

The textural qualities of the samples were measured using a micromeritics ASAP2010 analyzer (Thermo Scientific, USA). Brunauer-Emmett-Teller (BET) technique for adsorbent materials out gassing was performed on the sample. Moisture and volatiles that might impair the isotherms were removed overnight at 250 ± 1 °C in a vacuum. Following that, the sample was subjected to nitrogen at 77 K at various incremental pressures.

Determination of Degree of Deacetylation of Chitosan From Snail Shells

Using an agilent FTIR spectrometer, FTIR spectra of KBr pellets were measured in transmission mode in the region 4,000-650 cm^{-1} . Using the approach reported by Xu et al. (2019), DD of the samples was determined from IR spectra, as follows:

$$\%DD = 100 - \left[\frac{(A_{1837}/A_{3425}) \times 100}{1.33} \right], \text{ and}$$

$$\text{Absorbance (A)} = 2 - \text{Log}(\%T),$$

where DD is degree of deacetylation, A (A_{1837}) is absorbance band at 1,837 cm^{-1} , A_{3425} is absorbance band at 3,425 cm^{-1} , 1.33 denotes the factor of the ratio of A_{1837} to A_{3425} for fully N-acetylated CH and $\%T$ is the percentage transmittance.

Batch Adsorption Studies

The performance of adsorbents blends to remove chromium was evaluated using batch adsorption experiment as described by Upadhyay et al. (2021). The adsorption of Cr^{6+} was investigated by adding 1 g of adsorbent in an aqueous solution containing the desired concentrations of Cr (VI) of 20 mg/dm^3 to 150 mg/dm^3 . The pH of the solution was five, and it was shaken at 150 rpm for 72 hours at room temperature in a reciprocating shaker to equilibrate the system. The adsorption capacity or the equilibrium adsorption capacity per unit mass of the sample q_e (mgg^{-1}) and the removal was calculated, as follows:

$$q_e = \frac{(C_i - C_e)V}{W}$$

where V is volume of the solution in liters (l), W is weight of the adsorbent in grams (g), C_i is initial concentration (mg/dm^3), and C_e is equilibrium concentrations of adsorbate (mg/dm^3).

RESULTS AND DISCUSSION

The maximum yield of prepared CT and CH from snail shell were 63.48% and 57.15%, respectively. This shows that snail shell is good source of CH compared to other crustaceans like crabs and shrimps, which contain about 14.00%-26.00% and 17.00%-35.00%, respectively as reported by Olafadehan et al. (2021) and the yield depends on factors like the species of snail, reaction temperature, extraction time and concentration of acid and alkaline used (Sabir et al., 2019).

Characterization of Snail Shell, Chitin, & Chitosan

The characteristics of the snail shell and its derivatives with CC are given in **Table 1**. The weight on modification at the designated temperature yielded a high percentage of the adsorbents.

From **Table 1**, CH and chemically modified CH (CH_{ox}) were found to have pH values of 11.28 and 10.24, respectively, in slurry. The results obtained suggest that CH and CH_{ox} have basic surface functional groups (Pakizeh et al., 2021). There is an optimum pH of adsorbate in which the competition of hydrogen ions and metal precipitation are minimized hence, encouraging metal adsorption operation (Vu et al., 2019).

The bulk densities of CH and chemically modified CH (CH_{ox}) were the same, 0.58 g/cm^3 but slightly higher than CT (0.54 g/cm^3) and CC (0.49 g/cm^3). This proved that the modification process has negligible effect on their bulk densities of CH. The obtained values for adsorbents were favourable because they revealed that they were good adsorbents in terms of volume activity, since adsorption is a surface process. The experimental results agreed with 0.3g/ cm^3 reported by Asokogene et al. (2019) for CH from marine crab and squilla.

From **Table 1**, the experimental results of the moisture content and dry matter content of CH_T were determined to be 1.52% and 98.48%, respectively. This is favourable with CC of 1.08% and 98.92%. Also, results of the moisture content and dry matter content of CT were determined to be 4.18% and 95.82%, respectively. The percent moisture of (CH_{ox} 1.52%) agrees with 2.81% for CH reported by Sambo et al. (2019).

Table 1. Physico-chemical of adsorbents

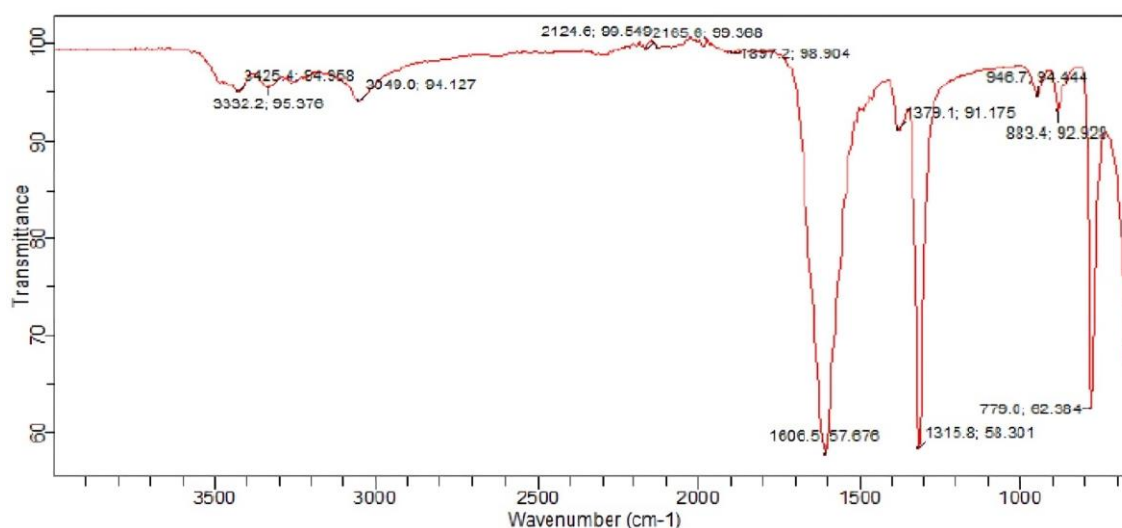
Adsorbent samples	pH of slurry at 28 °C	Bulk density (g/cm ³)	Moisture content (%)	Water binding capacity (%)	Ash content (%)	Conductivity (S/m)	Dry matter (%)
SSP	6.76	1.13	8.74	308.9	3.93	117.5	93.26
CT	8.47	0.54	4.18	319.7	1.68	117.8	95.82
CH	11.28	0.58	2.11	328.5	0.49	135.9	97.89
CH _{ox}	10.24	0.58	1.52	335.6	0.47	144.1	98.48
CC	8.58	0.49	1.08	462.5	0.87	310	98.92

Note. SSP: Snail shell particulates; CT: Chitin; CH: Chitosan; CH_{ox}: Oxalic acid modified chitosan; & CC: Commercial chitosan

Table 2. Surface textural properties of chitosan materials

Samples	BET surface area (m ² /g)	Mesoporosity (%)	DR Average pore width (nm)	Total pore volume (cm ³ /g)
SSP	356.34	71.18	6.366	0.1826
CT	282.99	71.38	6.247	0.1568
CH	362.32	71.41	6.214	0.2032
CH _{ox}	325.38	68.36	5.749	0.2000
CC	314.18	67.05	5.842	0.1891

Note. SSP: Snail shell particulates; CT: Chitin; CH: Chitosan; CH_{ox}: Oxalic acid modified chitosan; & CC: Commercial chitosan

**Figure 2.** FTIR transmittance spectrum of snail shell chitosan (CH) (Source: Authors' own elaboration)

From **Table 1**, the increasing order of WBC values of the adsorbents is SSP<CT<CH<CH_{ox}<CC. These values were between 295.30% and 462.50% and in agreement with similar studies on modified CH, which were reported to be in the range of 138.00% to 492.00% for CH synthesized from fish, crab, shrimp and mushroom (Fadhil & Mous 2021). However, the obtained results in this study are lower than the range, 458-805% documented by Asokogene et al. (2019) for CC from shrimps and crabs. Modifying and blending of the adsorbents tremendously increased WBC of the adsorbents.

From **Table 1**, the percentages of AC for adsorbents were found to be from 0.47% to 3.93%. The snail shell has the highest AC of 3.93% while CT has the lowest value (0.47%). The starting material for use as an adsorbent in wastewater treatment is better when it has lower AC. The values obtained for the samples were favourable because AC serves as interference during the adsorption (ElNasri et al., 2022). The results obtained for the prepared adsorbents were consistent with results reported by (da Silva Alves et al., 2021) for AC of CH (0.13%-32.40%).

The surface area is one of the most important characteristics of adsorbent and materials for other unit

operations. A large surface area is a requirement for good adsorbent. Their porosity enhances large surfaces area constituted by the pore walls (Mahmoodi et al., 2019). **Table 2** summarizes the textural characteristics of CH materials. Natural CH has a higher BET surface area and total pore volume than oxalic acid-modified CH (CH_{ox}) and CC. From **Table 2**, the increasing order of specific surface area is CT<CC<CH_{ox}<SSP<CH. The oxalic acid modification of CH (CH_{ox}) produces a mesoporous material with an average pore width of 5.749 nm and a surface area of 325.38 m²/g. These results are similar to CC with an average pore width of 5.842 nm a surface area of 314.18 m²/g whereas the CT was mesoporous material with an average pore width of 6.247 nm and a surface area of 282.99 m²/g (Francis et al., 2021).

Fourier Transform Infrared Spectral Analysis of Snail Shell Chitosan, Oxalic Acid Modified Chitosan, Commercial Chitosan, Chitin From Snail Shell, & Snail Shell Particulate

FTIR spectral of natural snail shell CH (**Figure 2**), oxalic acid modified CH CH_{ox} (**Figure 3**), CC (**Figure 4**), CT from snail shell CT, and SSP show the major bands assigned to different functional groups.

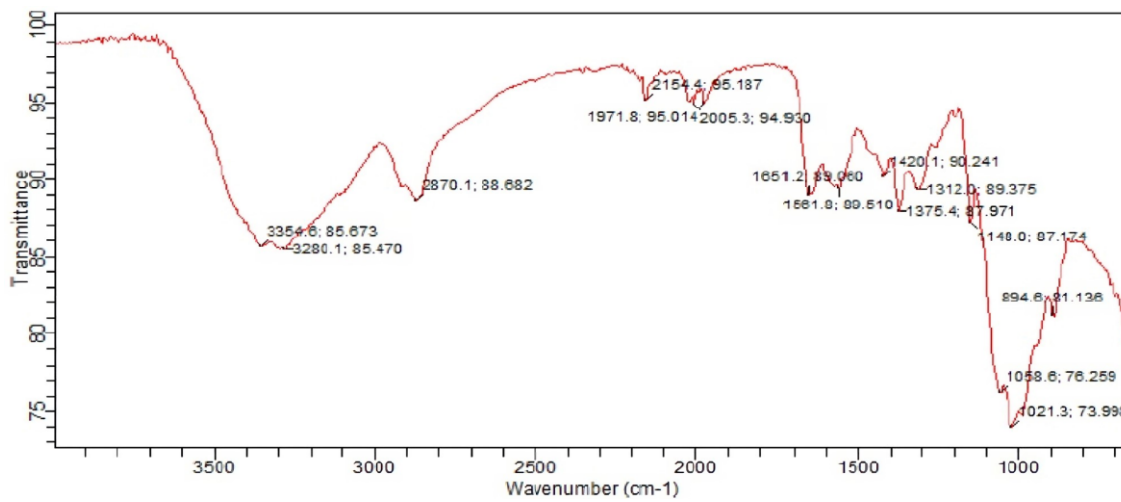


Figure 3. FTIR transmittance spectrum of oxalic acid modified chitosan (CH_{ox}) (Source: Authors' own elaboration)

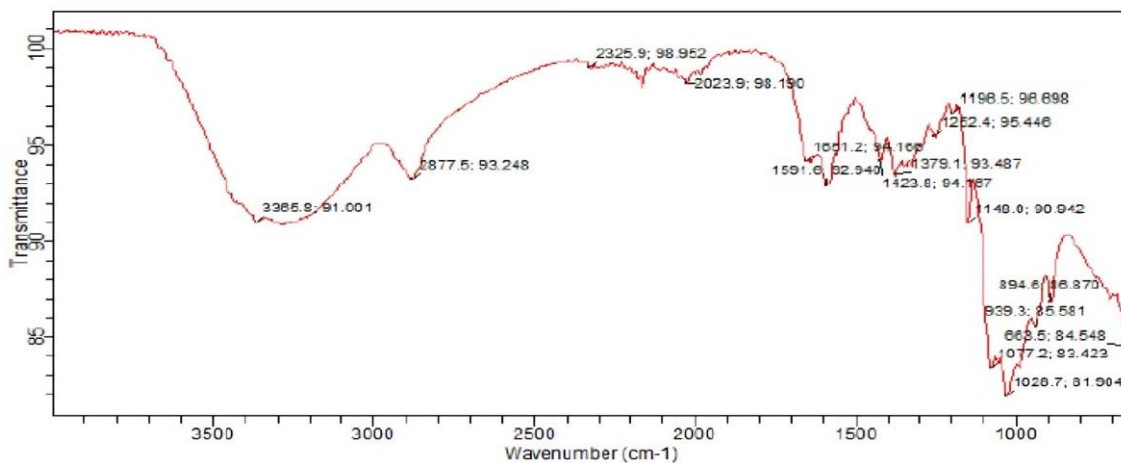


Figure 4. FTIR transmittance spectrum of commercial chitosan (CC) (Source: Authors' own elaboration)

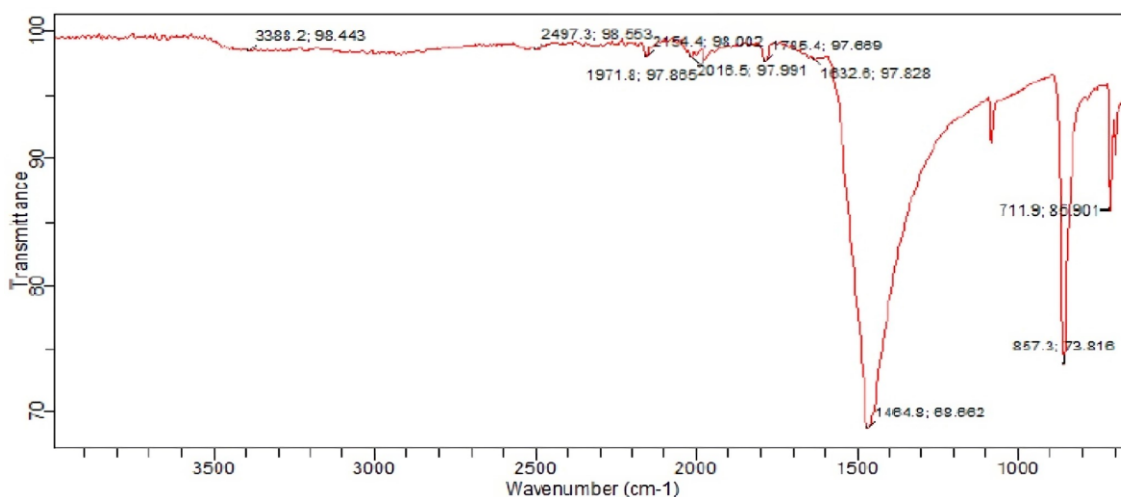


Figure 5. FTIR transmittance spectrum of chitin from snail shell (CT) (Source: Authors' own elaboration)

FTIR spectra of CH materials show absorption bands in region of 3,425.4-3,280.1 cm⁻¹ correspond to hydrogen joined O-H and N-H stretching vibrations primary and secondary amines/amides (Shin et al., 2019). Peaks at 3,049 and 2,800 cm⁻¹ are attributed to asymmetric and symmetric C-H stretching.

It was observed that there was shifting in the peaks between 2,154.6-1,897.2 cm⁻¹ assigned to C=C Alkyne and C≡N

Nitrile. Also, the band at 1,667-1,561.8 cm⁻¹ is attributed to C=C stretch aromatic and amide.

Stretching vibrations of -NH, -OH, -NH₂, and intermolecular hydrogen bonds that overlap each other might be assigned to characteristic band at 3,388.2 cm⁻¹ (Figure 5). The presence of the methyl group in NHC(O)CH₃ caused the observed peak at 2,154.4 cm⁻¹ and 2,018.5 cm⁻¹.

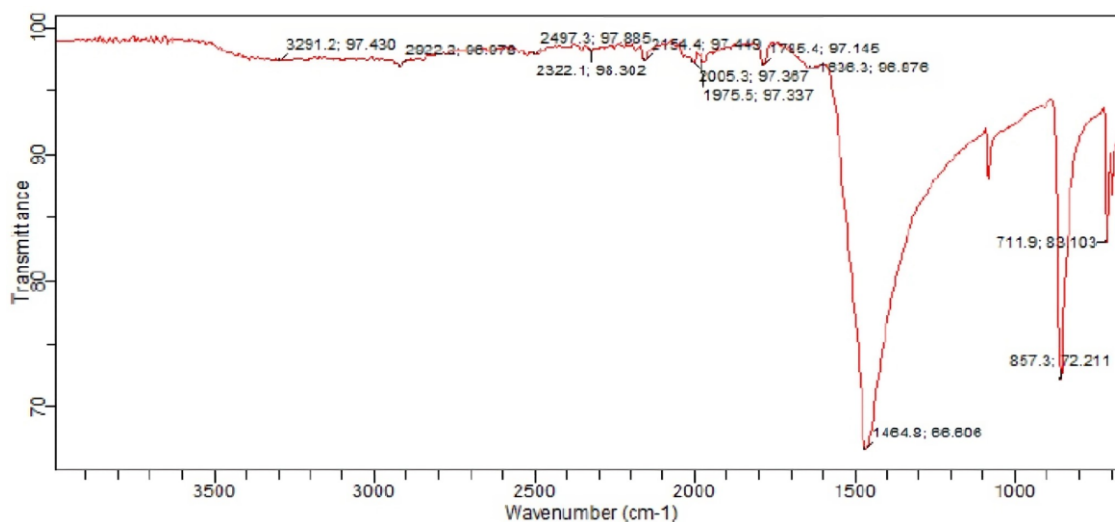


Figure 6. FTIR transmittance spectrum of snail shell particulate (SSP) (Source: Authors' own elaboration)

The existence of a carbonyl group at the observed band at $1,632.6\text{ cm}^{-1}$ aromatic ring fingerprint region was revealed by the characteristic -NH band of CT (Figure 5). The carbonyl group was formed as a result of presence of acetyl in CT. Amide II band (N-H bending) was suggested by the measured peak at $1,632.6\text{ cm}^{-1}$ (Barbosa et al., 2019). FTIR spectra of both CT and CH materials showcase the characteristics of primary and secondary amine/amide groups. The functional groups of CT and CH materials are revealed by FTIR spectra. All CH samples had equivalent peak characteristics, indicating that even after modification; the surface functional groups are similar (Madhu et al., 2022).

FTIR spectrum of SSP (Figure 6) shows the major bands assigned to different bonds. From Figure 6, the feature band at $3,291.2\text{ cm}^{-1}$ could be assigned to the stretching vibrations of -NH, -OH, and intermolecular hydrogen bonds, which overlap each other. The wave number at $2,922.2\text{ cm}^{-1}$ showed a functional group from stretching of C-H bonds of proteins, which may originate from the Snail metabolism. The $2,322.1\text{--}2,005.3\text{ cm}^{-1}$ bands showed the presence of an alkyne group, $\text{C}\equiv\text{C}$ and nitrile group, $\text{C}\equiv\text{N}$. It is also assigned that bands at around $1,975.5$ and $1,785.4\text{ cm}^{-1}$ were from carbonyl stretching of carbonate of aragonite or stretching of carbonyl of acidic proteins (Varma & Vasudevan, 2020).

Results of Degree of Deacetylation of Chitosan

DD of CH is a crucial property to consider because it affects its solubility, chemical reactivity, and biodegradability. Depending on the available source and approach, DD of CC can range from 30.00% to 95.00% (Nurhaeni et al., 2019). IR technique reported by Xu et al. (2019) was used to assess DD of CH from snail shell. A_{1837} and A_{3425} , respectively, are representations of the absorbance values at the wavelengths $1,837$ and $3,425\text{ cm}^{-1}$. For fully N-acetylated CH, the factor 1.33 represents the value of the ratio of A_{1837} to A_{3425} . From FTIR analysis of the prepared CH from snail shells, the percent transmittances at the wavelengths $1,837.2\text{ cm}^{-1}$ and $3,425.4\text{ cm}^{-1}$ were obtained. These values were then converted to absorbance (percent transmittance) from which the percentage of deacetylation was calculated to be 83.98%. Depending on the crustacean species and preparation

processes, DD of this study is higher than the ones reported by Koc et al. (2020) as 75.00%, 78.00%, and 70.00% for fish, shrimp, and crab CH, respectively. Also, Rajathy et al. (2021) found that *M. edulis* has a DD value of 69.60% and *L. attenuatum* has a DD value of 37.30%.

Results of Scanning Electron Microscopic Studies

SEM was used to determine the morphologies of the adsorbent surface. Figure 7 shows SEM images of CH material. CH has uneven patterns, which could be owing to flakes forming during the synthesis. The internal surfaces of the adsorbents have pores of various sizes, shapes, and fibril structures, while the external surfaces of the adsorbents have pores of various sizes, shapes, and fibril structures. Large numbers of intra-aggregated pores may result from the aggregation of these tiny primary nanoparticles, resulting in a large microporous volume. Tight porous, broken, and fibril structures are also present. The snail shell, CT and CH have well aggregated particles and a less porous look on the surface. Modification of the adsorbents caused the most significant changes. The structure of CH_{ox} is hard and organized, with minor fissures (Ochi et al., 2022; Rajathy et al., 2021).

Results of Energy Dispersive X-Ray Analysis

Figure 8 shows the EDAX spectra of CH compounds. EDAX was done to ascertain the sample elemental composition, as shown in Table 3. The spectra show prominent peaks for calcium (Ca), oxygen (O), and yttrium (Y). The intensity of the elements' peaks is similar in all samples, showing that minor changes in element composition occurred during the modification and composite synthesis but slightly different from CC. The elemental composition of commercial crab CH as described by Sumaila et al. (2020) is consistent with the presence of metals Ca, Y, Ag, Nb, K, Na, Mg, and Al in materials made from land snail shell CH. The mineral composition of gastropoda shells may be responsible for these alkaline metals, alkaline earth metals, rare earth metals, and transition metals (Angeli et al., 2021). In the meantime, Zhang et al. (2021) found that transition metals in adsorbents with concentrations ranging from 0.01% to 0.31% could improve the adsorption process.

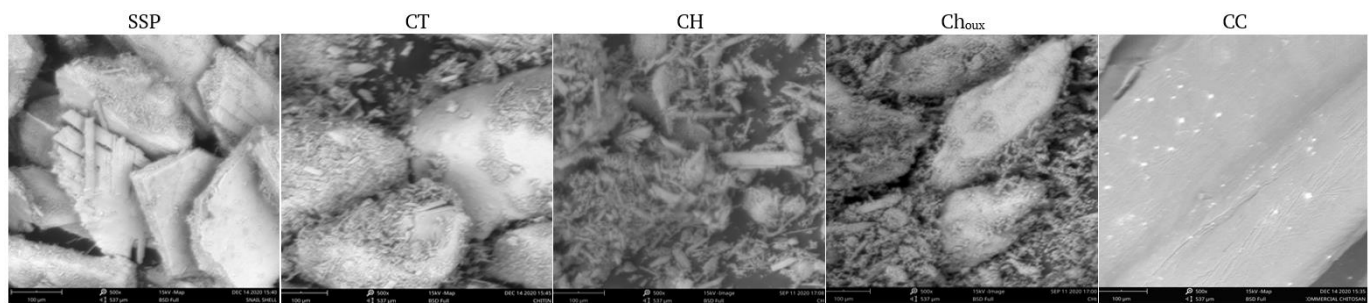


Figure 7. SEM images of SSP, CT, CH, CH_{ox}, & CC at 500X magnifications (Source: Authors' own elaboration)

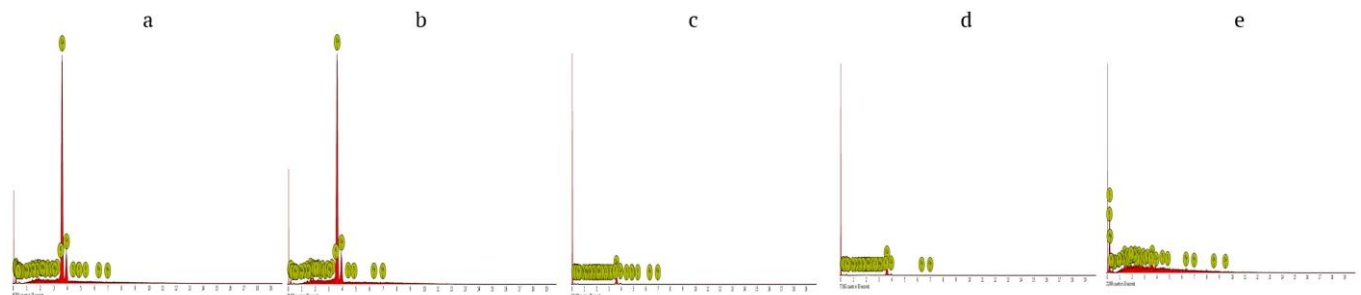


Figure 8. EDAX for elemental composition of (a) SSP, (b) CT, (c) CH, (d) CH_{ox}, & (e) CC (Source: Authors' own elaboration)

Table 3. EDAX for elemental composition of SSP, CT, & CH materials

ES	EN	Weight concentration of				
		SSP	CT	CH	CH _{ox}	CC
Ca	Calcium	88.19	85.66	70.43	64.88	10.46
O	Oxygen	3.84	2.80	16.74	23.32	0.00
Y	Yttrium	1.40	1.89	1.15	2.00	4.64
Ag	Silver	1.20	1.99	2.15	1.97	11.88
Nb	Niobium	1.13	1.70	1.27	1.58	9.05
K	Potassium	0.91	1.32	0.79	0.87	4.15
Cl	Chlorine	0.65	0.84	0.79	0.78	6.26
S	Sulfur	0.53	0.78	0.66	0.85	4.83
Si	Silicon	0.41	0.92	0.52	0.50	2.83
Al	Aluminum	0.41	0.61	0.62	0.67	4.62
C	Carbon	0.37	0.28	0.87	0.77	27.96
P	Phosphorus	0.28	0.23	0.98	0.29	3.93
Na	Sodium	0.26	0.21	0.61	0.16	1.74
Mg	Magnesium	0.24	0.31	0.30	0.34	2.93
N	Nitrogen	0.18	0.00	1.56	1.01	1.43
Fe	Iron	0.00	0.00	0.00	0.00	2.25
Ti	Titanium	0.00	0.46	0.17	0.00	1.05
V	Vanadium	0.00	0.00	0.39	0.00	0.00

Note. ES: Element symbol & EN: Element name

The chromium adsorption onto materials such as CT, CH, and snail shell particles is depicted in Figure 9.

The capacity to remove chromium often increased with concentration. It represents the function of heavy metal concentration to provide driving force to overcome solid mass transfer resistance for adsorption. The oxalic acid-modified CH exhibited the best adsorption capacity. The increasing order of the adsorption capacity is SSP < CT < CC < CH < CH_{ox}.

CH_{ox} has a better removal capacity of 80.5 mg/g at C₀=150 mg/l despite having a smaller surface area. However, while having a larger surface area, SSP has a fairly poor removal capacity because of its microporosity and pore size (6.366 nm), which would not be able to hold enough chromium ions. A

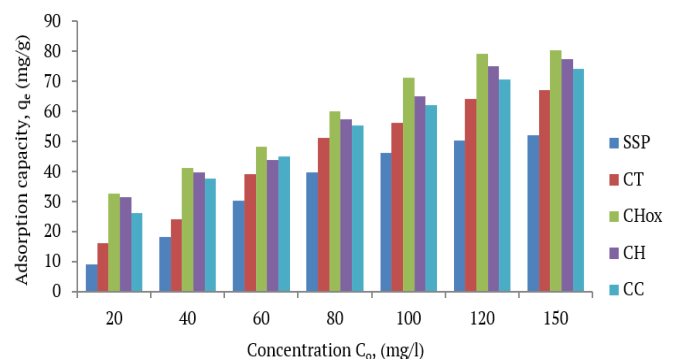


Figure 9. Chromium adsorption capacity of snail shell, chitin, & chitosan materials (Source: Authors' own elaboration)

superior performance of oxalic acid modified CH (CH_{ox}) and pure CH as compared with SSP, CT, and CC could be attributed to the enhanced surface chemistry by the deacetylation, modification process, specific surface area and mesoporosity. Ionic interaction between the negatively charged functional groups on the adsorbent surface and the positively charged metal ions, as well as mesopore filling, is the two potential mechanisms (Vu et al., 2019).

CONCLUSIONS

CH was prepared from the particulates of land snail shell and its product was modified with oxalic acid. The physico-chemical characteristics and chromium ion adsorption of CH materials were investigated. Functional groups like amino and O-H groups with hydrogen bonds suggest a potential adsorption interaction with positively charged water pollutants such as cationic heavy metal ions. After CH was modified, the textural characteristics, water binding, and adsorption capacity all significantly improved.

Some transition metals that are known to facilitate the adsorption process are present in CH compounds. Therefore, chromium ion adsorption on extracted natural and modified CH is slightly greater than CC but much higher than that on CT and particulate snail shells. This is because of the ionic interaction between the negatively charged functional groups on the adsorbent surface and the positively charged heavy metal, as well as the mesoporosity and increased surface area of the modified CH adsorbents.

Author contributions: All co-authors have been involved in all stages of this study while preparing the final version. They all agree with the results and conclusions.

Funding: This study was supported by the Tertiary Education Trust Fund of the Federal Republic of Nigeria through an Academic Staff Training and Development grant.

Declaration of interest: No conflict of interest is declared by the authors.

Ethical statement: The authors stated that the study did not require ethics committee approval since no live subjects were involved in the study.

Data sharing statement: Data supporting the findings and conclusions are available upon request from corresponding author.

REFERENCES

- Ahmed, M. J., Hameed, B., & Hummadi, E. H. (2020). Review on recent progress in chitosan/chitin-carbonaceous material composites for the adsorption of water pollutants. *Carbohydrate Polymers*, 247, 116690. <https://doi.org/10.1016/j.carbpol.2020.116690>
- Angeli, J. L. F., Sartoretto, J. R., Kim, B. S. M., de Lima Ferreira, P. A., de Mahiques, M. M., & Figueira, R. C. L. (2021). Trace element fluxes during the “anthropocene” in a large South American industrial and port area (Santos and Sao Vicente Estuarine System, SE, Brazil). *Environmental Monitoring and Assessment*, 193, 594. <https://doi.org/10.1007/s10661-021-09378-3>
- Asokogene, O. F., Zaini, M. A. A., Idris, M. M., Abdulsalam, S., & El-Nafaty, A. (2019). Physicochemical properties of oxalic acid-modified chitosan/neem leaves composites from Pessu River Crab Shell. *International Journal of Chemical Reactor Engineering*, 17(9), 20180274. <https://doi.org/10.1515/ijcre-2018-0274>
- ASTM International. (2019a). *Standard test methods for laboratory determination of water (moisture) content of soil and rock by mass*. <https://webstore.ansi.org/standards/astm/astme7097>
- ASTM International. (2019b). *Standard test method for pH of aqueous solutions with the glass electrode*. <https://www.astm.org/e0070-19.html>
- Barbosa, H. F. G., Francisco, D. S., Ferreira, A. P. G., & Cavalheiro, E. T. G. (2019). A new look towards the thermal decomposition of chitins and chitosans with different degrees of deacetylation by coupled TG-FTIR. *Carbohydrate Polymers*, 225, 115232. <https://doi.org/10.1016/j.carbpol.2019.115232>
- Chin, J. F., Heng, Z. W., Teoh, H. C., Chong, W. C., & Pang, Y. L. (2022). Recent development of magnetic biochar crosslinked chitosan on heavy metal removal from wastewater—Modification, application and mechanism. *Chemosphere*, 291, 133035. <https://doi.org/10.1016/j.chemosphere.2021.133035>
- da Silva Alves, D. C., Healy, B., Pinto L. A., Cadayal, T. R., & Breslin, C. B. (2021). Recent developments in chitosan-based adsorbents for the removal of pollutants from aqueous environments. *Molecules*, 26(3), 594. <https://doi.org/10.3390/molecules26030594>
- ElNasri, N. A., Wadidi, N. A., Idris, A. A. A., Woldemichael, S. K., & Ahmed El Haj, S. I. (2022). Properties of natural adsorbent prepared from two local Sudanese agricultural wastes mango seeds and date’s stones and their uses in removal of contamination from fluid nutrient. *Bulletin of the National Research Centre*, 46, 79. <https://doi.org/10.1186/s42269-022-00768-2>
- Fadhil, A., & Mous, E. F. (2021). Some characteristics and functional properties of chitin produced from local mushroom agaricus bisporus. *IOP Conference Series: Earth and Environmental Science*, 761, 012127. <https://doi.org/10.1088/1755-1315/761/1/012127>
- Francis, A. O., Zaini, M. A. A., Muhammad, I. M., Abdulsalam, S., & El-Nafaty, U. A. (2021). Physicochemical modification of chitosan adsorbent: A perspective. *Biomass Conversion and Biorefinery*, 13, 5557-5575. <https://doi.org/10.1007/s13399-021-01599-3>
- Gao, M., Tong, R., Huang, H., Kang, Y., Luo, Q., Huang, Y., & Chu, P. K. (2019). Activation of graphitic carbon nitride by surface discharge plasma treatment for enhanced photocatalysis. *Vacuum*, 159, 235-238. <https://doi.org/10.1016/j.vacuum.2018.10.038>
- Gulbis, A. (2019). *Big and small Roman snail*. <https://www.redzet.eu/en/photo/big-and-small-roman-snail-D-097-19>
- Hahn, T., Tafi, E., Paul, A., Salvia, R., Falabella, P., & Zibek, S. (2020). Current state of chitin purification and chitosan production from insects. *Journal of Chemical Technology & Biotechnology*, 95(11), 2775-2795. <https://doi.org/10.1002/jctb.6533>
- Hamli, H., Syed Azmai, S. H., Abdul-Hamed, S., & Abdulla-Al-Asif. (2019). Diversity and habitat characteristics of local freshwater gastropoda (caenogastropoda) from Sarawak, Malaysia. *Singapore Journal of Scientific Research*, 10(1), 23-27. <https://doi.org/10.3923/sjsres.2020.23.27>
- Hossain, S., & Uddin, K. (2020). Isolation and extraction of chitosan from shrimp shells. *International Journal of Advanced Research*, 8(9), 657-664. <https://doi.org/10.21474/IJAR01/11704>
- Huang, X., You, Z., Luo, Y., Yang, C., Ren, J., Liu, Y., Wei, G., Dong, P., & Ren, M. (2021). Antifungal activity of chitosan against phytophthora infestans, the pathogen of potato late blight. *International Journal of Biological Macromolecules*, 166, 1365-1376. <https://doi.org/10.1016/j.ijbiomac.2020.11.016>

- Keshvardoostchokami, M., Majidi, M., Zamani, A., & Liu, B. (2021). A review on the use of chitosan and chitosan derivatives as the bio-adsorbents for the water treatment: Removal of nitrogen-containing pollutants. *Carbohydrate Polymers*, 273, 118625. <https://doi.org/10.1016/j.carbpol.2021.118625>
- Khorshidi, N., Parsa, M., Lentz, D. R., & Sobhanverdi, J. (2021). Identification of heavy metal pollution sources and its associated risk assessment in an industrial town using the k-means clustering technique. *Applied Geochemistry*, 135, 105113. <https://doi.org/10.1016/j.apgeochem.2021.105113>
- Koc, B., Akyuz, L., Cakmak, Y. S., Sargin, I., Salaberria, A. M., Labidi, J., Ilk, S., Cekic, F. O., Akata, I., & Kaya, M. (2020). Production and characterization of chitosan-fungal extract films. *Food Bioscience*, 35, 100545. <https://doi.org/10.1016/j.fbio.2020.100545>
- Madhu, S., Devarajan, Y., Balasubramanian, M., & Raj, M. P. (2022). Synthesis and characterization of nano chitosan obtained using different seafood waste. *Materials Letters*, 329, 133195. <https://doi.org/10.1016/j.matlet.2022.133195>
- Mahmoodi, N. M., Mokhtari-Shourijeh, Z., & Abdi, J. (2019). Preparation of mesoporous polyvinyl alcohol/chitosan/silica composite nanofiber and dye removal from wastewater. *Environmental Progress & Sustainable Energy*, 38(s1), S100-S109. <https://doi.org/10.1002/ep.12933>
- Masselin, A., Rousseau, A., Pradeau, S., Fort, L., Gueret, R., Buon, L., Armand, S., Cottaz, S., Choisnard, L., & Fort, S. (2021). Optimizing chitin depolymerization by lysozyme to long-chain oligosaccharides. *Marine Drugs*, 19(6), 320. <https://doi.org/10.3390/md19060320>
- Morin-Crini, N., Lichtfouse, E., Torri, G., & Crini, G. (2019). Applications of chitosan in food, pharmaceuticals, medicine, cosmetics, agriculture, textiles, pulp and paper, biotechnology, and environmental chemistry. *Environmental Chemistry Letters*, 17, 1667-1692. <https://doi.org/10.1007/s10311-019-00904-x>
- Negm, N. A., Hefni, H., Abd-Elal, A. A., Badr, E. A., & Abou Kana, M. T. H. (2020). Advancement on modification of chitosan biopolymer and its potential applications. *International Journal of Biological Macromolecules*, 152, 681-702. <https://doi.org/10.1016/j.ijbiomac.2020.02.196>
- Nguyen, N. T. H., Long, V. D., & Fujita, T. (2023). A critical review of snail shell material modification for applications in wastewater, treatment. *Materials (Basel, Switzerland)*, 16(3), 1095. <https://doi.org/10.3390/ma16031095>
- Nurhaeni, Ridhay, A., Laenggeng, A. H. (2019). Optimization of degree of deacetylation of chitosan sail shells (pilla ampulaceae). *Asian Journal of Chemistry*, 31(9), 2083-2086. <https://doi.org/10.14233/ajchem.2019.22112>
- Ochi, D. O., Babayemi, A. K., & Ekebafé, L. O. (2022). Adsorbents characterization and effect of reaction indices on the uptake of cadmium (II) and chromium (VI) ions from wastewater. *Nigerian Journal of Chemical Research*, 27(1), 1-18.
- Olafadehan, O., Kehinde, O. A., Tolulase, O. A., & Bello, V. E. (2021). Extraction and characterization of chitin and chitosan from callinectes amnicola and penaeus notialis shell wastes. *Journal of Chemical Engineering and Materials Science*, 12(1), 1-30. <https://doi.org/10.5897/JCEMS2020.0353>
- Oyekunle, D. T., & Omoleye, J. A. (2019a). Effect of particle sizes on the kinetics of demineralised of snail shell for chitin synthesis using acetic acid. *Heliyon*, 5(11), e02828. <https://doi.org/10.1016/j.heliyon.2019.e02828>
- Oyekunle, D. T., & Omoleye, J. A. (2019b). New process for synthesizing chitosan from snail shells. *Journal of Physics: Conference Series*, 1299(1), 012089. <https://doi.org/10.1088/1742-6596/1299/1/012089>
- Pakizeh, M., Moradi, A., & Ghassemi, T. (2021). Chemical extraction and modification of chitin and chitosan from shrimp shells. *European Polymer Journal*, 159, 110709. <https://doi.org/10.1016/j.eurpolymj.2021.110709>
- Rajathy, T. J., Srinivasan, M., & Mohanraj, T. (2021). Physicochemical and functional characterization of chitosan from horn snail gastropod telescopium telescopium. *Journal of Applied Pharmaceutical Science*, 11(2), 52-58.
- Rathore, B. S., Chauhan, N. P. S., Jadoun, S., Ameta, S. C., & Ameta, R. (2021). Synthesis and characterization of chitosan-polyaniline nickel (II) oxide nanocomposite. *Journal of Molecular Structure*, 1242, 130750. <https://doi.org/10.1016/j.molstruc.2021.130750>
- Sabir, A., Altaf, F., & Shafiq, M. (2019). Synthesis and characterization and application of chitin and chitosan-based eco-friendly polymer composites. In S. T. Inamuddin, R., Mishra, & A. Asiri (Eds.), *Sustainable polymer composites and nanocomposites* (pp. 1365-1405). Springer. https://doi.org/10.1007/978-3-030-05399-4_46
- Samarah, N., Al-Quraan, N., Massad, R., & Welbaum, G. (2020). Treatment of bell pepper (capsicum annum L.) seeds with chitosan increases chitinase and glucanase activities and enhances emergence in a standard cold test. *Scientia Horticulturae*, 269, 109393. <https://doi.org/10.1016/j.scienta.2020.109393>
- Sambo, R. E., Nuhu, A. A., & Uba, S. (2019). Preparation and characterisation of shrimp waste-derived chitin, chitosan and modified chitosan films. *Nigerian Research Journal of Chemical Sciences*, 6, 213-230.
- Shin, C. S., Kim, D. Y., & Shin, W. S. (2019). Characterization of chitosan extracted from mealworm beetle (tenebrio molitor, zophobas morio) and rhinoceros beetle (allomyrina dichotoma) and their antibacterial activities. *International Journal of Biological Macromolecules*, 125, 72-77. <https://doi.org/10.1016/j.ijbiomac.2018.11.242>
- Singh, A., Sharma, A., Verma, R. K., Chopade, R. L., Pandit, P. P., Nagar, V., Aseri, V., Choudhary, S. K., Awasthi, G., Awasthi, K. K., & Sankhla, M. S. (2022). Heavy metal contamination of water and their toxic effect on living organisms. In D. J. Dorta, & D. P. de Oliveira (Eds.), *The toxicity of environment of pollutants*. IntechOpen. <https://doi.org/10.5772/intechopen.105075>

- Sirajudheen, P., Poovathumkuzhi, N. C., Vigneshwaran, S., Chelaveettil, B. M., & Meenakshi, S. (2021). Applications of chitin and chitosan based biomaterials for the adsorptive removal of textile dyes from water—A comprehensive review. *Carbohydrate Polymers*, 273, 118604. <https://doi.org/10.1016/j.carbpol.2021.118604>
- Sumaila, A., Ndamitso, M. M., Iyaka, Y.A., Abdulkareem, A. S., Tijani, J. O., & Idris, M. O. (2020). Extraction and characterization of chitosan from crab shells: Kinetic and thermodynamic studies of arsenic and copper adsorption from electroplating wastewater. *Iraqi Journal of Science*, 61(9), 2156-2171. <https://doi.org/10.24996/ijs.2020.61.9.2>
- Thasneema, K.K., Dipin, T., Thayyil, M. S., Sahu, P.K., Messali, M., Rosalin, T., Elyas, K., Saharuba, P., Anjitha, T., & Ben Hadda, T. (2020). Removal of toxic heavy metals, phenolic compounds and textile dyes from industrial wastewater using phosphonium based ionic liquids. *Journal of Molecular Liquids*, 323, 114645. <https://doi.org/10.1016/j.molliq.2020.114645>
- Upadhyay, U., Sreedhar, I., Singh, S. A., Patel, C. M., & Anitha, K. L. (2021). Recent advances in heavy metal removal by chitosan based adsorbents. *Carbohydrate Polymers*, 251, 117000. <https://doi.org/10.1016/j.carbpol.2020.117000>
- Vakili, M., Deng, S., Cagnetta, G., Wang, W., Meng, P., Liu, D., & Yu, G. (2019). Regeneration of chitosan-based adsorbents used in heavy metal adsorption: A review. *Separation and Purification Technology*, 224, 373-387. <https://doi.org/10.1016/j.seppur.2019.05.040>
- Varma, R., & Vasudevan, S. (2020). Extraction, characterization, and antimicrobial activity of chitosan from horse mussel *modiolus modiolus*. *ACS Omega*, 5, 20224-20230. <https://doi.org/10.1021/acsomega.0c01903>
- Vinod, A., Sanjay, M. R., Suchart, S., & Jyotishkumar, P. (2020). Renewable and sustainable biobased materials: An assessment on biofibers, biofilms, biopolymers and biocomposites. *Journal of Cleaner Production*, 258, 120978. <https://doi.org/10.1016/j.jclepro.2020.120978>
- Vu, X. H., Nguyen, L. H., Van, H. T., Nguyen, D. V., Nguyen, T. H., Nguyen, Q. T., & Ha, L. T. (2019). Adsorption of chromium (VI) onto freshwater snail shell-derived biosorbent from aqueous solutions: Equilibrium, kinetics, and thermodynamics. *Journal of Chemistry*, 2019, 3038103. <https://doi.org/10.1155/2019/3038103>
- Wang, J., & Zhuang, S. (2022). Chitosan-based materials: Preparation, modification and application. *Journal of Cleaner Production*, 355, 131825. <https://doi.org/10.1016/j.jclepro.2022.131825>
- Xu, J., Liu, L., Yu, J., Zou, Y., Wang, Z., & Fan, Y. (2019). DDA (degree of deacetylation) and pH-dependent antibacterial properties of chitin nanofibers against *escherichia coli*. *Cellulose*, 26, 2279-2290. <https://doi.org/10.1007/s10570-019-02287-2>
- Yadav, M., Goswami, P., Paritosh, K., Kumar, M., Pareek, N., & Vivekanand, V. (2019). Seafood waste: A source for preparation of commercially employable chitin/chitosan materials. *Bioresources and Bioprocessing*, 6, 8. <https://doi.org/10.1186/s40643-019-0243-y>
- Zazycki, M. A., Borba, P. A., Silva, R. N. F., Peres, E. C., Perondi, D., Collazzo, G. C., & Dotto, G. L. (2019). Chitin derived biochar as an alternative adsorbent to treat colored effluents containing methyl violet dye. *Advanced Powder Technology*, 30(8), 1494-1503. <https://doi.org/10.1016/j.appt.2019.04.026>
- Zhang, Y., Zhao, M., Cheng, Q., Wang, C., Li, H., Han, X., Fan, Z., Su, G., Pan, D., & Li, Z. (2021). Research progress of adsorption and removal of heavy metals by chitosan and its derivatives: A review. *Chemosphere*, 279, 130927. <https://doi.org/10.1016/j.chemosphere.2021.130927>